THE JOURNAL OF PHYSICAL CHEMISTRY C

Article

Cite This: J. Phys. Chem. C 2020, 124, 398−403

pubs.acs.org/JPCC

Hydration Energetics of a Diamine-Appended Metal−Organic Framework Carbon Capture Sorbent

Jun Wang,[†,‡,§,⋈] Esra Yılmaz,[‡,§,#,⋈] Xianghui Zhang,[‡,§] Houqian Li,[§] Renqin Zhang,[▽] Xiaofeng Guo,[‡,∥,⊥] Hui Sun,[*,○,◆] Baodong Wang,[¶] and Di Wu[*,‡,§,∥,⊥]

[†]School of Physics and Electronic Engineering, Sichuan University of Science and Engineering, Zigong, Sichuan 643036, China

[‡]Alexandra Navrotsky Institute for Experimental Thermodynamics, [§]The Gene and Linda Voiland School of Chemical Engineering and Bioengineering, [∥]Department of Chemistry, and [⊥]Materials Science and Engineering, Washington State University, Pullman, Washington 99163, United States

[#]Department of Chemical Engineering, Ege University, İzmir 35100, Turkey

[▽]McKetta Department of Chemical Engineering, University of Texas, Austin, Texas 78712, United States

[○]Petroleum Processing Research Center and [◆]International Joint Research Center of Green Energy Chemical Engineering, East China University of Science and Technology, Shanghai 200237, China

[¶]National Institute of Clean-and-Low-Carbon Energy, Beijing 102211, China

ABSTRACT: mmen-Mg_2(dobpdc) (mmen = *N,N′*-dimethylethylenediamine, dobpdc = 4,4′-dioxidobiphenyl-3,3′-dicarboxylate) is a diamine-appended metal−organic framework (MOF) material with promising future as an efficient CO_2 capture sorbent for industry applications. Here, using adsorption calorimetry, the energetic landscape of mmen-Mg_2(dobpdc) hydration has been revealed. Specifically, at near-zero water coverage, hydration results in the most exothermic differential enthalpy of adsorption of −110.9 ± 3.1 kJ/mol water. A differential enthalpy plateau at −65.8 ± 4.7 kJ/mol water is observed at the intermediate degree of hydration, which corresponds to water−diamine chemisorption through hydrogen bonding. Eventually, mmen-Mg_2(dobpdc) hydration is concluded at the second differential enthalpy plateau at −44.2 ± 1.8 kJ/mol water suggesting condensation of water within the internal channel space of mmen-Mg_2(dobpdc). The position of the second plateau at about −44.0 kJ/mol water strongly suggests formation of liquid-like water clusters within the hydrophilic nanoconfinement environment. This comprehensive study energetically distinguishes the guest−host interfacial bonding and guest−guest intermolecular interactions for the water−mmen-Mg_2(dobpdc) system, which provides fundamental thermodynamic data to enhance our understanding of the behavior of CO_2 capture sorbents in the presence of moisture.

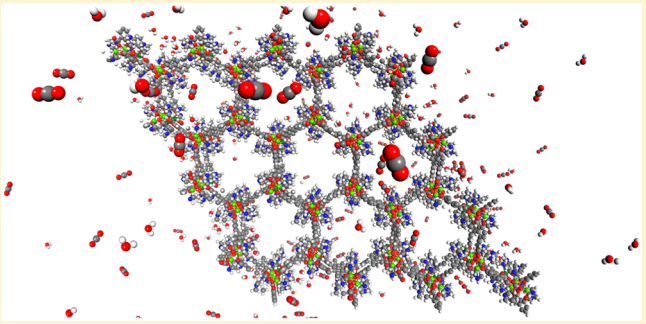

INTRODUCTION

Metal−organic frameworks (MOFs)-based materials have great potential to be applied as sorbents for adsorptive separation of gas[1−4] or liquid mixtures,[5−8] such as carbon capture,[2,9] alkane/alkene separation,[10−13] organosulfur elimination,[7] and noble gas mixtures separation.[14−16] MOFs are a family of crystalline porous materials, constructed through coordination between metal nodes and organic linkers.[17] Their open framework structures with large surface area feature accessible metal sites and tunable linkers, both of which can be further modified to introduce chemical functionalities. One example is a diamine-appended MOF, *N,N′*-dimethylethylenediamine (mmen)-Mg_2(dobpdc), (dobpdc = 4,4′-dioxidobiphenyl-3,3′-dicarboxylate), which exhibits complex "first-order phase transition-like" metal site−amine cooperative insertion binding mechanism leading to step-shape CO_2 sorption isotherms with high working capacity.[18,19] Interestingly, the "step" of each isotherm right-shifts significantly as temperature increases.[18,19] While its CO_2 capture performance and adsorption energetics have been thoroughly investigated,[19,20] the thermodynamics of water−mmen-Mg_2(dobpdc) interactions remains undocumented. Moreover, considering the metastability of MOF-based materials under humid conditions, and potential applications of mmen-Mg_2(dobpdc) in industrial settings, it is essential and critical to understand its hydration properties.

Degradation of MOFs under humid conditions[21] and decreased CO_2 adsorption capacity in the presence of moisture have been reported.[22,23] On the other hand, in numerous studies, it has been observed that hydration affected CO_2

Received: August 21, 2019
Revised: November 26, 2019
Published: December 9, 2019

DOI: 10.1021/acs.jpcc.9b08008
J. Phys. Chem. C 2020, 124, 398−403

capture capacity. For example, Liu et al. reported a significantly decreased CO_2 adsorption capacity for Mg_2(dobdc) (1,4-dioxido-2,5-benzenedicarboxylate) when it was exposed to steam.[22] Chen et al. examined the role of water in CO_2 capture on both hydrated and dehydrated MIL-101 (Cr).[24] Interestingly, they found that the water molecules in hydrated MIL-101 (Cr) acted as additional CO_2 adsorption sites, which led to increased CO_2 uptake at low pressure. Moreover, it has been reported that a 5-fold increase in CO_2 adsorption capacity on MIL-100 (Fe) was seen at 40% of relative humidity.[25] For mmen-Mg_2(dobpdc), Long and his colleagues thoroughly investigated its CO_2 capture performance in the presence of moisture.[26] Specifically, Fourier transform infrared (FTIR) results suggested that water did not impact the cooperative insertion mechanism of CO_2 capture. Surprisingly, they also found that for mmen-Ni_2(dobpdc), one member of the mmen-M_2(dobpdc) family did not adsorb CO_2 through cooperative insertion, exhibited "hydration-boosted" CO_2 capture capacity. They attributed such enhancement to the formation of bicarbonates and/or alkyl ammonium carbamate species. This phenomenon was highlighted by Jones and colleagues.[27] These studies point out the critical role of water in governing CO_2 capture performance and mechanisms. However, experimental thermodynamic studies on sorbent hydration energetics and mechanisms using calorimetry are rarely reported.

Adsorption calorimetry has been primarily applied to study the surface energetics of nanoparticles and nuclear materials and binding site distribution within porous materials and on catalyst surface.[29−32] A typical setup includes a Calvet microcalorimeter coupled with a commercial gas adsorption analyzer (see Figure 1a). Recently, we applied this methodology to study the adsorption energetics of CO_2 capture on two MOFs, a sugar MOF, cyclodextrin-MOF-2 (CD-MOF-2),[33] and a diamine-appended MOF, mmen-Mg_2(dobpdc).[20] The general phenomenon found is that incremental dosing of CO_2 to the sorbent from high vacuum results in (1) very exothermic initial binding at near-zero coverage and subsequent (2) differential enthalpy curve with plateau(s), with each plateau indicating binding sites of the same energetic state.[29] Additionally, in 2016, we reported a water adsorption calorimetry study on the hydration energetics of Cu-HKUST-1, in which complex interplay of pore/channel confinement and surface binding at copper nodes was revealed. Most interestingly, it was found that the concluding stage of hydration appears to be on hydrophobic surfaces.[28] In this study, we applied water adsorption calorimetry to investigate the hydration energetics of mmen-Mg_2(dobpdc) (see Figure 1b). Specifically, the water adsorption enthalpies were directly measured at 25 °C and plotted as a function of the degree of hydration (water loading). Further, integrated with results from thermogravimetry−differential scanning calorimetry−mass spectrometry (TG−DSC−MS), we were able to interpret the hydration mechanism of mmen-Mg_2(dobpdc) and discussed the evolutions of partial molar properties, including differential entropy and chemical potential change of hydration as water loading varies.

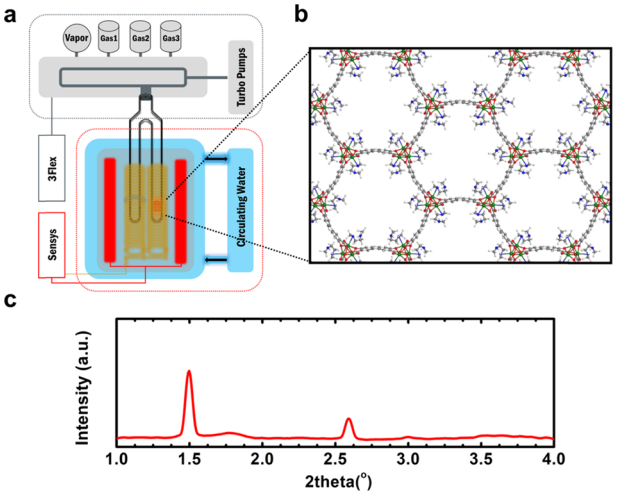

Figure 1. (a) Schematics of the adsorption calorimetry system, (b) molecular structure, and (c) room-temperature small-angle X-ray scattering (SAXS) patterns of mmen-Mg_2(dobpdc).

EXPERIMENTAL METHODS

Material Synthesis. To synthesize mmen-Mg_2(dobpdc), we applied the strategy reported by McDonald et al.[18] Specifically, $Mg(NO_3)_2{\cdot}6H_2O$ (65 mg), H_4dobpdc (28 mg), and a solvent (10 mL of 55/45 v/v methanol/dimethylformamide mixture) were mixed in a glass scintillation vial (20 mL). This vial was then sealed with a poly(tetrafluoroethylene) (PTFE) cap and transferred into a six-hole aluminum alloy well plate placed on a heating plate. After heating at 120 °C for 12 h, the precipitate was soaked in and washed with dimethylformamide and methanol five times. The solid product was collected and degassed at 250 °C under vacuum overnight to obtain Mg_2(dobpdc). The mmen-grafting process was performed in a dry nitrogen-filled glovebox. 10% mmen/hexane solution (10 mL) was dripped into a Micromeritics sample tube containing activated Mg_2(dobpdc) (∼100 mg). The final product, mmen-Mg_2(dobpdc), was collected, vacuum-filtered, and washed with dry hexane five times. The residual hexane was removed by heating the sample at 100 °C under vacuum overnight.[19]

Materials Characterization. Small-angle X-ray scattering (SAXS) was performed to identify the structure of mmen-Mg_2(dobpdc). The SAXS pattern was collected at the B1 station of Cornell High Energy Synchrotron Source (CHESS) using an angle dispersive synchrotron X-ray technique. In each measurement, the white X-ray beams were collimated into the monochromatic beam at a wavelength of 0.485946 Å using a double crystal monochromator, and a large MAR345 detector was employed to monitor the X-ray scattered signals. In addition, all two-dimensional (2D) images were converted to one-dimensional (1D) patterns with intensity as a function of 2θ (degree) for structural analysis by using a Fit2D software.[34] Diffuse reflectance infrared Fourier transform spectroscopy (DRIFTS) experiments were carried out under helium flow (40 cm^3/min) using a Bruker Tensor 27 IR spectrometer equipped with a Praying Mantis diffuse reflection accessory by Harrick Scientific Products. Potassium bromide (KBr) was used as the background material. Spectra were collected at 30 and 100 °C from 4000 to 500 cm^{-1} at 4 cm^{-1} to verify the success of mmen-grafting.

Water Adsorption Calorimetry. The hydration enthalpies of mmen-Mg_2(dobpdc) at 25 °C were measured using a customized adsorption calorimetry system, which featured a gas dosing manifold (Micromeritics 3Flex) integrated with a Calvet-type microcalorimeter (Setaram Sensys Evo).[35] In our experiments, the mmen-Mg_2(dobpdc) was hydrated "in situ" in

DOI: 10.1021/acs.jpcc.9b08008
J. Phys. Chem. C 2020, 124, 398−403

the calorimeter from high vacuum. About 20 mg of mmen-Mg_2(dobpdc) was loaded on one side of a home-made silica glass forked tube. The other side of the tube remained empty serving as a reference. This sample tube was introduced into the calorimeter, connected with the gas dosing port, and degassed under vacuum (<10^{-6} mmHg) at 100 °C for 24 h to remove any presorbed species. During the calorimetry measurements, 3Flex, the gas dosing system, dosed water vapor incrementally. Each dose introduced ∼1 μmol of water vapor with at least 2 h gap to ensure that the adsorption reached thermodynamic equilibrium, which was evidenced by a horizontally flat baseline. Each adsorption equilibrium led to a corresponding calorimetric signal (peak). The adsorption isotherm and associated heat effects were monitored and recorded simultaneously. Integration of the area under the calorimetric peak returned the total heat effect (kJ) of a particular dose (mole of adsorbate). Using these two sets of data, we were able to calculate the differential enthalpies of adsorption with the unit kJ per mole of the adsorbate (kJ/mol adsorbate). We used a Calisto Processing software (AKTS, Switzerland) for peak area integration and data analysis.

Thermogravimetry–Differential Scanning Calorimetry–Mass Spectrometry (TG–DSC–MS). TG–DSC–MS analysis was performed using a STA 449 F3 Jupiter (Netzsch Instrument) coupled with a quadrupole mass spectrometer QMS 403 D (Aëolos) to elucidate the dehydration and decomposition processes of hydrated mmen-Mg_2 (dobpdc) in air. A sample pellet, ∼10 mg, was placed in a Pt crucible and heated from 35 to 600 °C at 10 °C per min under air flow (20 cm^3/min). The evolved gases were analyzed simultaneously by the MS, in which signals of water (m/z = 18) and CO_2 (m/z = 44) were recorded.

RESULTS AND DISCUSSION

The 1D SAXS pattern of mmen-Mg_2(dobpdc) is presented in Figure 1c, in which three major peaks are identified with d-spacings of 1.86 nm (d_1), 1.07 nm (d_2), and 0.93 nm (d_3). Their corresponding d_1/d_n ratios are approximately 1, $\sqrt{3}$, and 2. Such geometry strongly suggests a 2D hexagonal superstructure.[36] Considering the mesoporosity of mmen-Mg_2(dobpdc), the first three peaks in Figure 1c are indexed as (10), (11), and (20). Further, we calculated the lattice constant of mmen-Mg_2(dobpdc) (2.15 nm) using the following equation.[36]

$$\frac{1}{d_{hk}^2} = \frac{4}{3}\frac{h^2 + hk + k^2}{a^2}$$

DRIFTS data were collected to ensure the success of mmen–metal coordination (see Figure 2). After heating at 100 °C, two well-resolved peaks are observed between 3400 and 3200 cm^{-1}, which correspond to the stretching vibration modes of grafted (3259 cm^{-1}) and free (3328 cm^{-1}) N–H groups[37] of the mmen molecule. The bands between 2800 and 3000 cm^{-1} are assigned to the methylene stretching[37] of the mmen molecule.[18,19] The peaks found at about 1630 and 1590 cm^{-1} are probably due to the carbamate C=O stretching modes.[38] There is also a well-resolved IR band at about 1334 cm^{-1} owing to the vibrational mode of C–N within carbamate,[38,39] which is the product of CO_2 cooperative insertion in mmen-Mg_2(dobpdc). This set of data is a strong evidence suggesting the success in grafting of mmen molecules at the metal sites of Mg_2(dobpdc). Moreover, it also details the

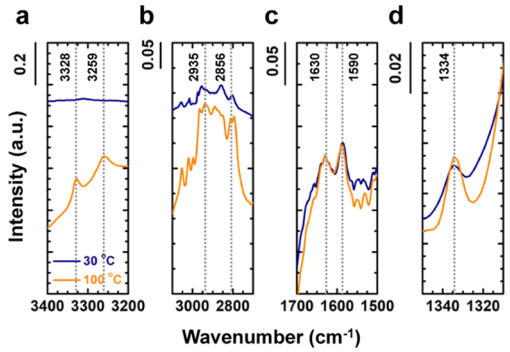

Figure 2. DRIFTS spectra of mmen-Mg_2(dobpdc) at 30 °C (navy) and 100 °C (orange) in helium flow. (a) Range of wavenumber 3400–3200 cm^{-1}, (b) 3100–2700 cm^{-1}, (c) 1700–1500 cm^{-1}, and (d) 1400–1300 cm^{-1}.

bonding changes during the CO_2 desorption process, in which the vibration modes of N–H groups become better resolved as the temperature increases. In contrast, mmen-Mg_2(dobpdc) with both CO_2 and water adsorbed presents weak amine IR signals at 30 °C.

The water adsorption isotherm and differential enthalpy of hydration (enthalpy change per mole of water) profile are plotted in Figure 3a,b, respectively. We also include the CO_2

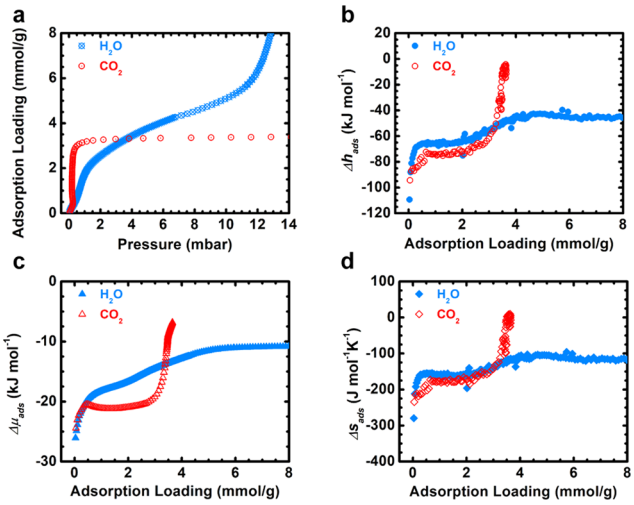

Figure 3. (a) Water and CO_2 adsorption isotherms and corresponding (b) differential enthalpies, (c) chemical potential, and (d) differential entropies of adsorption plots at 25 °C on mmen-Mg_2(dobpdc).[20]

adsorption isotherm at 25 °C and corresponding thermodynamic data for comparison.[20] The triplicated water adsorption isotherms are overlapped, which suggests good reproducibility. The most exothermic near-zero coverage differential enthalpy of hydration is −110.9 ± 3.1 kJ/mol water, which is more exothermic than that of CO_2 adsorption, −94.4 ± 2.8 kJ/mol CO_2.[20] Subsequently, the differential enthalpy of hydration curve tends to be less exothermic and switches to a plateau at −65.8 ± 4.7 kJ/mol water. This plateau starting from ∼0.2 mmol/g suggests strong hydrogen bonding between water and the amine groups of mmen-Mg_2(dobpdc). Notably, at an uptake of 3.5 mmol/g, CO_2 adsorption becomes energetically less favorable (less exothermic) compared with hydration. At about 4.0 mmol/g, the differential enthalpy of the hydration

DOI: 10.1021/acs.jpcc.9b08008
J. Phys. Chem. C 2020, 124, 398–403

curve gently reaches its second plateau at −44.2 ± 1.8 kJ/mol water. The magnitude of this heat effect strongly suggests condensation of water within the hydrophilic confinement environment of mmen-Mg_2(dobpdc).

To further reveal the thermodynamic insights into mmen-Mg_2(dobpdc) hydration as a function of water loading, we derive other partial molar properties of water adsorption, including chemical potential (differential free energy) and differential entropy of hydration (see Figure 3c,d). In our earlier study, we choose pure CO_2 at 1 atm and 25 °C as the standard state.[20] In this study, the chemical potential (partial molar free energy) is derived from the water adsorption isotherm using the equation $\Delta\mu = RT\ \ln(p/p^o)$, in which p/p^o is the relative pressure of water vapor. The choice of the standard state for a particular adsorption system does not impact the results of our analysis because what we obtain is the difference between the initial state (preadsorption of a specific dose) and the final state (postadsorption equilibrium of that dose). We use the chemical potential and directly measured differential enthalpy of hydration data to calculate the partial molar hydration entropy using the following relation: $\Delta\mu_{ads} = \Delta h_{ads} - T\Delta s_{ads}$.

The chemical potential mimics the fashion of differential enthalpy of hydration profile. Specifically, $\Delta\mu_{ads}$ appears to be less negative as more water is loaded. At near-zero coverage, the steep increase in both differential enthalpy and chemical potential of hydration highlights the strong thermodynamic driving force of initial water−mmen-Mg_2(dobpdc) binding. Meanwhile, the partial molar hydration entropy tends to be less negative as water loading increases. This indicates that the dynamics of water confined within mmen-Mg_2(dobpdc) channels appears to be bulk water-like. Such a phenomenon has not been observed in our earlier study on thermodynamics of Cu-HKUST-1 hydration, which has much more hydrophobic surfaces.[31]

Furthermore, we separate the differential entropy of hydration into two terms, one corresponding to (1) the entropy change due to pressure increase, $\Delta s_{pressure} = -R\ \ln p$, the other (2) purely originates from hydration, $\Delta s_{adsorption} = \Delta h_{adsorption}/T$. The results are plotted in Figure 4, in which pressure increase leads to entropy increases, while adsorption results in more ordered, liquid-like water adsorbed on the sorbent surface and confined within the pore space of mmen-Mg_2(dobpdc), leading to entropy decrease.

The TG−DSC−MS results of hydrated mmen-Mg_2(dobpdc) in air flow are presented in Figure 5. There

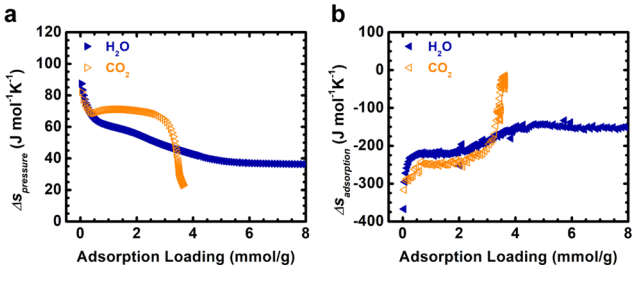

Figure 4. Differential entropies of water adsorption on mmen-Mg_2(dobpdc) at 25 °C. (a) Contribution from gas/vapor expansion from water saturation pressure, P_o, to the pressure, P, of the adsorption isotherm and (b) contribution purely from adsorption (hydration). The CO_2 data from our earlier study are also plotted for comparison.[20]

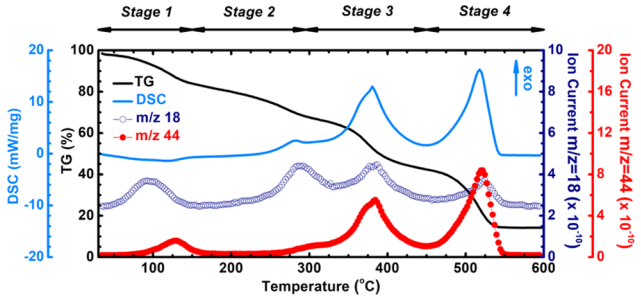

Figure 5. TG−DSC−MS profiles of mmen-Mg_2(dobpdc) in air flow from 30 to 600 °C. The TG and DSC curves are black and light blue, respectively. The MS data of water and CO_2 are plotted in navy circle and red dots, respectively.

appears to be a four-stage weight loss mechanism. Specifically, in stage 1, between 35 and 150 °C, the sample loses about 15% of its weight, resulting in a broad endothermic peak due to dehydration and desorption of CO_2 picked up once exposed to ambient conditions (see Figure 5, m/z = 18 and 44). In stage 2, further dehydration between 150 and 295 °C accounts for another ∼15% weight loss leading to an endothermic heat event. Subsequently, in stages 3 and 4, the sample experiences a two-step highly exothermic combustion accompanied with simultaneous liberation of water and CO_2. Particularly, stage 3 decomposition ranges from 295 to 450 °C showing a sharp exothermic peak centered at 397 °C, which is very likely due to combustion of mmen. After 450 °C, all organic species, primarily the organic linkers of Mg_2(dobpdc), are fully oxidized to water and CO_2 in stage 4. The TG−DSC−MS results synchronize well with the water adsorption calorimetry data, both of which highlight the presence of two groups of energetically distinctive water in hydrated mmen-Mg_2(dobpdc), including chemisorbed water and loosely confined physisorbed water. The populations of these two types of water are approximately the same, according to the isotherm and TG−DSC−MS data. The delayed presence of the first two water peaks in the MS profiles is due to the dynamic nature of TG−DSC−MS thermal analysis and diffusion resistance from the sorbent.

In light of the calorimetric results, we are able to interpret the hydration mechanism of mmen-Mg_2(dobpdc). First, the differential enthalpy, entropy, and chemical potential of water adsorption all point out that the hydration of mmen-Mg_2(dobpdc) has three distinctive steps, including (i) near-zero coverage water binding on the most favorable sites, (ii) water adsorption at the majority amine groups through hydrogen bonding (the first plateau), and (iii) water−water intermolecular interactions under pore confinement. In general, (i) and (ii) are classified as guest−host interfacial interactions, while (iii) is categorized as guest−guest intermolecular interactions under nanoconfinement. This is distinctly different from what we have found for CO_2 capture on mmen-Mg_2(dobpdc), in which only adsorbate−adsorbent binding was detected. This is because at near-room temperature and pressure below 1 bar, CO_2 does not have significant intermolecular interactions, whereas water molecules tend to bind themselves through hydrogen bonding. As a result, water−water interactions (clustering and/or condensation) are particularly severe under nanoconfinement in materials with mesoporosity and hydrophilic surfaces. In sharp contrast, hydration of hydrophobic MOFs and solid-state oxides usually

DOI: 10.1021/acs.jpcc.9b08008
J. Phys. Chem. C 2020, 124, 398−403

returns differential enthalpy of hydration much less exothermic than −44.0 kJ/mol water.[28,32] In other words, water molecules tend to fill channels or pores with hydrophilic surfaces, yet they form highly dynamic metastable clusters within hydrophobic environments.

This calorimetric study highlights a few unique hydration properties of mmen-Mg_2(dobpdc). The condensation is very likely to result in pore blockage leading to poor gas transport and sorbent degradation. In summary, the fundamental calorimetric study provides comprehensive thermodynamic insights governing the complex interactions among water, CO_2, and mmen-Mg_2(dobpdc).

CONCLUSIONS

In this study, we applied water adsorption calorimetry as a fundamental tool to study the thermodynamics of mmen-Mg_2(dobpdc) hydration. We found that beyond the near-zero coverage binding (−110.9 ± 3.1 kJ/mol water), mmen-Mg_2(dobpdc) hydration is stepwise featuring two distinctive stages representing water−amine interfacial binding (−65.8 ± 4.7 kJ/mol water) and water−water intermolecular interactions (condensation) in pores (−44.2 ± 1.8 kJ/mol water). Further, the chemical potential and partial molar entropy evolutions of mmen-Mg_2(dobpdc) hydration were derived from the calorimetry results and discussed, which mirror favorable hydration on a hydrophilic sorbent. This set of hydration thermodynamics data is complementary to the existing CO_2 capture studies on mmen-Mg_2(dobpdc), which aids our fundamental understanding of the energetics of hydration related to CO_2 capture on mmen-M_2(dobpdc) (M: metal) sorbents.

AUTHOR INFORMATION

Corresponding Authors

*E-mail: sunhui@ecust.edu.cn (H.S.).
*E-mail: d.wu@wsu.edu (D.W.).

ORCID

Xiaofeng Guo: 0000-0003-3129-493X
Hui Sun: 0000-0002-8544-756X
Di Wu: 0000-0001-6879-321X

Notes

The authors declare no competing financial interest.
⋈J.W. and E.Y. contributed equally.

ACKNOWLEDGMENTS

This work was supported by the institutional funds from the Gene and Linda Voiland School of Chemical Engineering and Bioengineering at Washington State University. D.W. and X.G. acknowledge the fund of Alexandra Navrotsky Institute for Experimental Thermodynamics. X.Z. is supported by Chambroad Scholarship. H.S. acknowledges the funds from the National Natural Science Foundation of China (Grants 91634112 and 21878097), the Natural Science Foundation of Shanghai (Grant 16ZR1408100), and the Open Project of State Key Laboratory of Chemical Engineering (SKL-ChE-16C01). J.W. acknowledges the Key Project of Education Department of Sichuan Province (15ZA0229) and the Youth Talent Oversea Support Program of Sichuan University of Science and Engineering. The Cornell High Energy Synchrotron Source is supported by National Science Foundation Award DMR0936384.

REFERENCES

(1) Jiang, J.; Furukawa, H.; Zhang, Y. B.; Yaghi, O. M. High Methane Storage Working Capacity in Metal-Organic Frameworks with Acrylate Links. *J. Am. Chem. Soc.* **2016**, *138*, 10244−10251.
(2) Zheng, B.; Yun, R.; Bai, J.; Lu, Z.; Du, L.; Li, Y. Expanded Porous MOF-505 Analogue Exhibiting Large Hydrogen Storage Capacity and Selective Carbon Dioxide Adsorption. *Inorg. Chem.* **2013**, *52*, 2823−2829.
(3) Avci, G.; Velioglu, S.; Keskin, S. High-Throughput Screening of MOF Adsorbents and Membranes for H2 Purification and CO2 Capture. *ACS Appl. Mater. Interfaces* **2018**, *10*, 33693−33706.
(4) Wu, D.; Guo, X.; Sun, H.; Navrotsky, A. Thermodynamics of Methane Adsorption on Copper HKUST-1 at Low Pressure. *J. Phys. Chem. Lett.* **2015**, *6*, 2439−2443.
(5) Sarker, M.; Song, J. Y.; Jhung, S. H. Carboxylic-Acid-Functionalized UiO-66-NH2: A Promising Adsorbent for Both Aqueous- and Non-Aqueous-Phase Adsorptions. *Chem. Eng. J.* **2018**, *331*, 124−131.
(6) Li, C.; Xiong, Z.; Zhang, J.; Wu, C. The Strengthening Role of the Amino Group in Metal-Organic Framework MIL-53 (Al) for Methylene Blue and Malachite Green Dye Adsorption. *J. Chem. Eng. Data* **2015**, *60*, 3414−3422.
(7) Sun, H.; Han, X.; Liu, K.; Shen, B.; Liu, J.; Wu, D.; Shi, X. Metal-Modified Cu-BTC Acid for Highly Enhanced Adsorption of Organosulfur Species. *Ind. Eng. Chem. Res.* **2017**, *56*, 9541−9550.
(8) Yılmaz, E.; Sert, E.; Atalay, F. S. Synthesis, Characterization of a Metal Organic Framework: MIL-53 (Fe) and Adsorption Mechanisms of Methyl Red onto MIL-53 (Fe). *J. Taiwan Inst. Chem. Eng.* **2016**, *65*, 323−330.
(9) Lu, C. M.; Liu, J.; Xiao, K.; Harris, A. T. Microwave Enhanced Synthesis of MOF-5 and Its CO2 Capture Ability at Moderate Temperatures across Multiple Capture and Release Cycles. *Chem. Eng. J.* **2010**, *156*, 465−470.
(10) Sun, H.; Ren, D.; Kong, R.; Wang, D.; Jiang, H.; Tan, J.; Wu, D.; Chen, S.; Shen, B. Tuning 1-Hexene/n-Hexane Adsorption on MOF-74 via Constructing Co-Mg Bimetallic Frameworks. *Microporous Mesoporous Mater.* **2019**, *284*, 151−160.
(11) Li, L.; Guo, L.; Pu, S.; Wang, J.; Yang, Q.; Zhang, Z.; Yang, Y.; Ren, Q.; Alnemrat, S.; Bao, Z. A Calcium-Based Microporous Metal-Organic Framework for Efficient Adsorption Separation of Light Hydrocarbons. *Chem. Eng. J.* **2019**, *358*, 446−455.
(12) Wang, X.; Krishna, R.; Li, L.; Wang, B.; He, T.; Zhang, Y. Z.; Li, J. R.; Li, J. Guest-Dependent Pressure Induced Gate-Opening Effect Enables Effective Separation of Propene and Propane in a Flexible MOF. *Chem. Eng. J.* **2018**, *346*, 489−496.
(13) Sun, H.; Jiang, H.; Kong, R.; Ren, D.; Wang, D.; Tan, J.; Wu, D.; Zhu, W.; Shen, B. Tuning N-Alkane Adsorption on Mixed-Linker ZIF-8-90 via Controllable Ligand Hybridization: Insight into the Confinement from an Energetics Perspective. *Ind. Eng. Chem. Res.* **2019**, *58*, 13274−13283.
(14) Greathouse, J. A.; Kinnibrugh, T. L.; Allendorf, M. D. Adsorption and Separation of Noble Gases by IRMOF-1: Grand Canonical Monte Carlo Simulations. *Ind. Eng. Chem. Res.* **2009**, *48*, 3425−3431.
(15) Lee, S. J.; Yoon, T. U.; Kim, A. R.; Kim, S. Y.; Cho, K. H.; Hwang, Y. K.; Yeon, J. W.; Bae, Y. S. Adsorptive Separation of Xenon/Krypton Mixtures Using a Zirconium-Based Metal-Organic Framework with High Hydrothermal and Radioactive Stabilities. *J. Hazard. Mater.* **2016**, *320*, 513−520.
(16) Dorcheh, A. S.; Denysenko, D.; Volkmer, D.; Donner, W.; Hirscher, M. Noble Gases and Microporous Frameworks; From Interaction to Application. *Microporous Mesoporous Mater.* **2012**, *162*, 64−68.
(17) Wu, D.; Navrotsky, A. Thermodynamics of Metal-Organic Frameworks. *J. Solid State Chem.* **2015**, *223*, 53−58.
(18) McDonald, T. M.; Mason, J. A.; Kong, X.; Bloch, E. D.; Gygi, D.; Dani, A.; Crocellà, V.; Giordanino, F.; Odoh, S. O.; Drisdell, W. S.; et al. Cooperative Insertion of CO2 in Diamine-Appended Metal-Organic Frameworks. *Nature* **2015**, *519*, 303−308.

DOI: 10.1021/acs.jpcc.9b08008
J. Phys. Chem. C 2020, 124, 398−403

(19) McDonald, T. M.; Lee, W. R.; Mason, J. A.; Wiers, B. M.; Hong, C. S.; Long, J. R. Capture of Carbon Dioxide from Air and Flue Gas in the Alkylamine-Appended Metal-Organic Framework Mmen-Mg 2(Dobpdc). *J. Am. Chem. Soc.* **2012**, *134*, 7056−7065.
(20) Wu, D.; McDonald, T. M.; Quan, Z.; Ushakov, S. V.; Zhang, P.; Long, J. R.; Navrotsky, A. Thermodynamic Complexity of Carbon Capture in Alkylamine-Functionalized Metal-Organic Frameworks. *J. Mater. Chem. A* **2015**, *3*, 4248−4254.
(21) Tan, K.; Nijem, N.; Canepa, P.; Gong, Q.; Li, J.; Thonhauser, T.; Chabal, Y. J. Stability and Hydrolyzation of Metal Organic Frameworks with Paddle-Wheel SBUs upon Hydration. *Chem. Mater.* **2012**, *24*, 3153−3167.
(22) Liu, J.; Benin, A. I.; Furtado, A. M. B.; Jakubczak, P.; Willis, R. R.; Levan, M. D. Stability Effects on CO_2 Adsorption for the DOBDC Series of Metal Organic Frameworks. *Langmuir* **2011**, *27*, 11451−11456.
(23) Yu, J.; Balbuena, P. B. Water Effects on Postcombustion Co_2 Capture in Mg-MOF-74. *J. Phys. Chem. C* **2013**, *117*, 3383−3388.
(24) Chen, Y. F.; Babarao, R.; Sandler, S. I.; Jiang, J. W. Metal - Organic Framework MIL-101 for Adsorption and Effect of Terminal Water Molecules: From Quantum Mechanics to Molecular Simulation. *Langmuir* **2010**, *26*, 8743−8750.
(25) Soubeyrand-lenoir, E.; Vagner, C.; Yoon, J. W.; Bazin, P.; Ragon, F.; Hwang, Y. K.; Serre, C.; Chang, J.; Llewellyn, P. L. How Water Fosters a Remarkable 5-Fold Increase in Low-Pressure. *J. Am. Chem. Soc.* **2012**, *134*, 10174−10181.
(26) Mason, J. A.; McDonald, T. M.; Bae, T. H.; Bachman, J. E.; Sumida, K.; Dutton, J. J.; Kaye, S. S.; Long, J. R. Application of a High-Throughput Analyzer in Evaluating Solid Adsorbents for Post-Combustion Carbon Capture via Multicomponent Adsorption of CO_2, N_2, and H_2O. *J. Am. Chem.Soc.* **2015**, *137*, 4787−4803.
(27) Darunte, L. A.; Walton, K. S.; Sholl, D. S.; Jones, C. W. CO2 Capture via Adsorption in Amine-Functionalized Sorbents. *Curr. Opin. Chem. Eng.* **2016**, *12*, 82−90.
(28) Wu, D.; Guo, X.; Sun, H.; Navrotsky, A. Interplay of Confinement and Surface Energetics in the Interaction of Water with a Metal-Organic Framework. *J. Phys. Chem. C* **2016**, *120*, 7562−7567.
(29) Li, G.; Sun, H.; Xu, H.; Guo, X.; Wu, D. Probing the Energetics of Molecule-Material Interactions at Interfaces and in Nanopores. *J. Phys. Chem. C* **2017**, *121*, 26141−26154.
(30) Guo, X.; Wu, D.; Ushakov, S. V.; Shvareva, T.; Xu, H.; Navrotsky, A. Energetics of Hydration on Uranium Oxide and Peroxide Surfaces. *J. Mater. Res.* **2019**, *34*, 3319−3325.
(31) Wu, D.; Guo, X.; Sun, H.; Navrotsky, A. Interplay of Confinement and Surface Energetics in the Interaction of Water with a Metal-Organic Framework. *J. Phys. Chem. C* **2016**, *120*, 7562−7567.
(32) Wu, D.; Guo, X.; Sun, H.; Navrotsky, A. Energy Landscape of Water and Ethanol on Silica Surfaces. *J. Phys. Chem. C* **2015**, *119*, 15428−15433.
(33) Wu, D.; Gassensmith, J. J.; Gouveîa, D.; Ushakov, S.; Stoddart, J. F.; Navrotsky, A. Direct Calorimetric Measurement of Enthalpy of Adsorption of Carbon Dioxide on CD-MOF-2, a Green Metal-Organic Framework. *J. Am. Chem. Soc.* **2013**, *135*, 6790−6793.
(34) Hammersley, A. P.; Svensson, S. O.; Hanfland, M.; Fitch, A. N.; Hausermann, D. Two-Dimensional Detector Software: From Real Detector to Idealised Image or Two Theta Scan. *High Pressure Res.* **1996**, *14*, 235−248.
(35) Ushakov, S. V.; Navrotsky, A. Direct Measurements of Water Adsorption Enthalpy on Hafnia and Zirconia. *Appl. Phys. Lett.* **2005**, *87*, No. 164103.
(36) Hahn, T. et al. *International Tables for Crystallography*; Dordrecht: Reidel, 2002; Vol. *1*, pp 128.
(37) Bernini, M. C.; Blanco, A. A. G.; Sapag, K.; Narda, G. E.; et al. Tuning the Target Composition of Amine-Grafted CPO-27-Mg for Capture of CO2 under Post-Combustion and Air Filtering Conditions: A Combined Experimental and Computational Study. *Dalton Trans.* **2015**, *44*, 18970−18982.
(38) Vlaisavljevich, B.; Odoh, S. O.; Schnell, S. K.; Dzubak, A. L.; Lee, K.; Planas, N.; Neaton, J. B.; Gagliardi, L.; Smit, B. CO2 induced phase transitions in diamine- appended metal−organic frameworks. *Chem. Sci.* **2015**, *6*, 5177−5185.
(39) Siegelman, R. L.; Mcdonald, T. M.; Gonzalez, M. I.; Martell, D.; Milner, P. J.; Mason, J. A.; Berger, A. H.; Bhown, A. S.; Long, R. Controlling Cooperative CO_2 Adsorption in Diamine-Appended Mg 2 (Dobpdc) Metal − Organic Frameworks. *J. Am. Chem. Soc.* **2017**, *139*, 10526−10538.

DOI: 10.1021/acs.jpcc.9b08008
J. Phys. Chem. C 2020, 124, 398−403